Comprehensive analysis of retroreflection in *Papilio crino* Fabricius, 1792 wings

Juliet Sackey[1,2] ✉, Kwadwo A. Dompreh[1,3], Malik Maaza[1,2]

[1]Nanosciences African Network (NANOAFNET), iThemba LABS-National Research Foundation, Old Faure Road,7129, Somerset West, South Africa
[2]UNESCO-UNISA Africa Chair in Nanosciences/Nanotechnology, College of Graduate Studies, University of South Africa (UNISA), Muckleneuk Ridge, P.O. Box 392, Pretoria, South Africa
[3]Department of Physics, University of Cape Coast, Ghana
✉ E-mail: jsackeyunisa@gmail.com

Abstract: Multilayer thin-film structures in the wings of a butterfly; *Papilio crino* produce a colourful iridescence from reflected light. In this investigation, scanning electron microscope images show both the concave cover scales and pigmented air-chamber ground scales. The microstructures with the concavities retroreflect incident light, thus causing the double reflection. This gives rise to both the colour mixing and polarisation conversion clearly depicted in the optical images. The result of the numerical and theoretical analysis via the CIELAB, and optical reflection and transmission of light through the multilayer stacks with the use of transfer method show that the emerging colouration on the *Papilio crino* is structural and is due to the combination of colours caused by multiple bounces within the concavities. The butterfly wing structure can be used as the template for designing the photonic device.

1 Introduction

The beautiful colour patterns observed on butterfly wings rise from the interaction of light on the periodic nano-scale structures [1–4]. The replication of these colours has gained considerable attention in the biomimicry industry due to the many applications derived from such study. A combination of multi-layer interference, diffraction gratings, photonic crystals and other optical structures in several Lepidoptera species gives rise to the bright colours [5–7] useful for the creation of model systems to better understand structural colours. Generally, the wings scales of the butterflies, particularly the papailioned consist of regular deformed multilayer structures that are made from alternating layers of air and cuticle which create intense structural colours.

Currently, researchers have identified the colour producing structures in several of the Papilionoideae species such as *P. blumei*, *P. palinurus* and *P. Buddha* [8, 9]. In recent studies, Vukusic *et al.* [10] examined the scales of the *P. palinurus* to consist of an array of concavities exhibiting two distinct colours on the edges and the incline sides. In their analysis, they described in details the optical response and plane polarisation on the wings scales. In addition, they illustrated that the pairs of inclined surfaces with almost identical multilayers had matched the spectral reflectivity characteristics which produce the intense blue reflectivity through double reflection. Similar studies show that the scales exhibit non-planar specular reflection as a different colour for different angles [11, 12].

One characteristic identical to this papilionidae is iridescence [13]. The colour produced by the wing structure changes over a wide range of the human visible spectrum depending on the viewing direction. As established, the iridescence on the wings of butterflies is due to interference, scattering and diffraction caused by the multilayers [14].

Against this background, we focused on the interaction of light on the wing concavity as displayed by the cover scale of *Papilio crino*. The conspicuously large size butterfly; *Papilio crino* [15] indigenous to Central and Southern India [16] exhibits this characteristic. To our knowledge, there is no comprehensive optical study on this species; hence in this study, we show through experimental, numerical and computational modelling that the

concavities (as will be seen in the scanning electron microscope – SEM images) induce a polarisation rotation caused by phase shift between TE and TM polarised reflections. In the analysis, we show that the emerging colouration on the *Papilio crino* is structural and is due to the combination of colours caused by multiple bounces within the concavities.

2 Morphological characterisation

For this investigation, the part of the wing showing the colour of interest was cut and attached to a sample holder using carbon taps. It was later coated with thin gold-palladium ultra-layer (25 Å) in order to prevent electron charging. Once coated, it was imaged by Carl Zeiss Auviga SEM operated at 5 keV.

The SEM images of the dorsal view of the *Papilio crino* wing displaying the arrangement of the scales are shown in Fig. 1*a*. The two distinct layers; the cover scales consist of an ordered array of concavities while the ground scales are decorated with nanometre-sized air chambers. Both scales have ridges separated by cross-ribs but different scale shapes. The results of the particle size distribution analysis (PSDA) give an approximation of the predominating circular cross-ribs on all the images and also their different diameters (sizes). The polynomial fit of the frequency to the diameter of the circular cross-ribs is estimated in the frequency plots (see Fig. 1*b*) and the resulting equations presented.

The Fourier transform images (see Fig. 1*c*) clearly reveal the ridges with their periodicities, respectively. The diffused disks in the reciprocal space identified on all the images could originate from the nanometre air chambers in the real space images.

Figs. 2*a* and *b* show the curved multilayers below the round concavity consisting of about eight alternate layers of cuticle and air (Fig. 2*a*) and schematic representation (Fig. 2*b*).

3 Optical images

The CIELAB colour space illustrates the colours perceived on the wings of the *Papilio crino* (see Fig. 3). The CIE colour model is a mapping system that uses tristimulus (a combination of three colour values that are close to red/green/blue) values [17]. It is one of the models that describe the entire range of colours the human
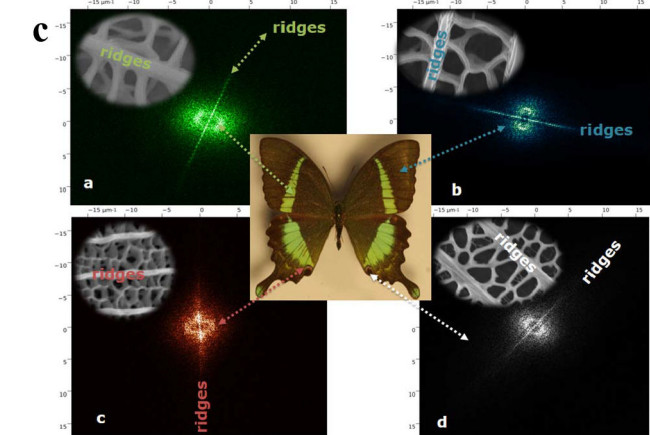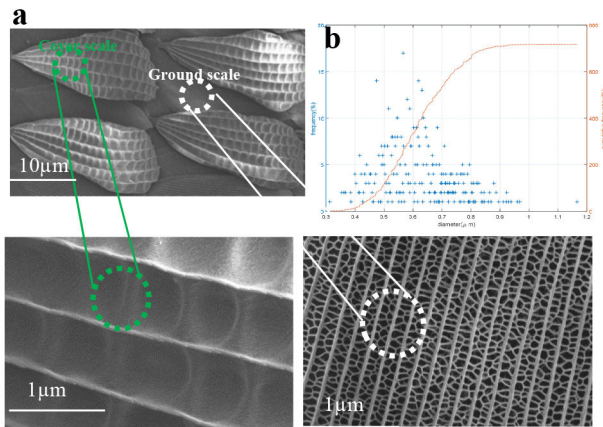
Fig. 1 *Morphological and optical images of the dorsal view of the Papilio crino wing*
(a) SEM images showing the two types of scales; cover and ground scales. Concavities are clearly seen on the cover scale separating the ridges while nanostructured air chambers are identical to the ground scale, *(b)* Frequency plot showing the overall number of particles as ∼699 with an average diameter of 0.617 µm. The coefficient of the polynomial fit of the frequency to the diameter is $p(x) = -0.0001x^3 + 0.0045x^2 - 0.0487x + 0.7519$, *(c)* 2D FFT images (a–d) of the *Papilio crino*

eye can see. In this study, the illuminate D65 is used with the k-means cluster algorithm in Matlab to define the colours. CIE XYZ tristimulus values were calculated from reflectance spectra and then converted to the sRGB colour space. The results indicate that the colours perceived by the eye are actually a combination of colours being reflected off the microstructures on the scales. Placing the wing between the polarisers, the reflection of light off the centre of the cavities is suppressed while the retroreflected light from four segments of the cavity edge is detected [12] (see Fig. 4). At an angle of 45°, the reflected light is blue, highly polarised and goes out after double reflection in the direction of the incidence (see Fig. 4*c*).

4 Optical characterisation

A reflection probe with small tips from Avantes enlightening spectroscopy made of six illumination fibres around a single read fibre was used for the reflectance measurement. The single fibre leg was connected to the spectrometer (AvaSpec-ULS2048L StarLine Versatile Fibre-optic Spectrometer) for the detection and the other end was connected to the deuterium halogen source (AvaLight-DH-S). To measure the reflectance at the different angles, firstly, the probe end was directed through the reflection probe holder (AFH-15 angle fibre holder) and focused on the reference material. The WS-2 reference tile made of a white PTFE-based material considered as the highest grade reference material for diffuse reflectance was used as the reference material, the shutter was closed and the detector screened from light when
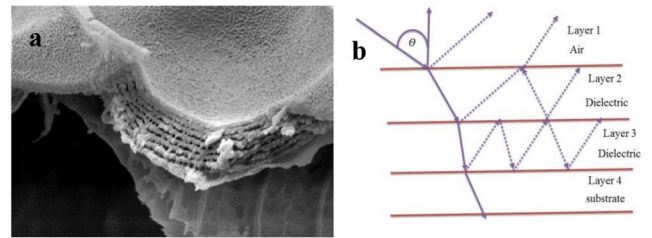

Fig. 2 *SEM image of cross-section of dorsal view of the Papilio crino wing*
(a) SEM image of the scale showing a multilayer stack of the scale, *(b)* Schematic representations of incident light propagation at an angle through the multilayer stack
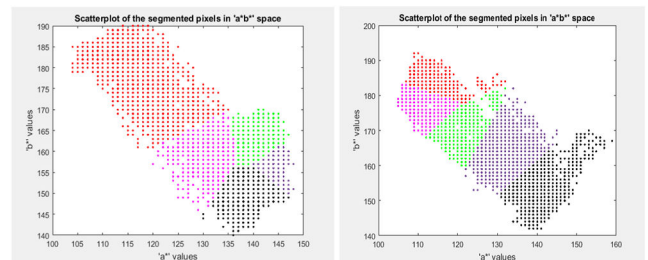

Fig. 3 *L.a.b colour space of the segmented upper part of the wing (left) and that of the lower part (right)*
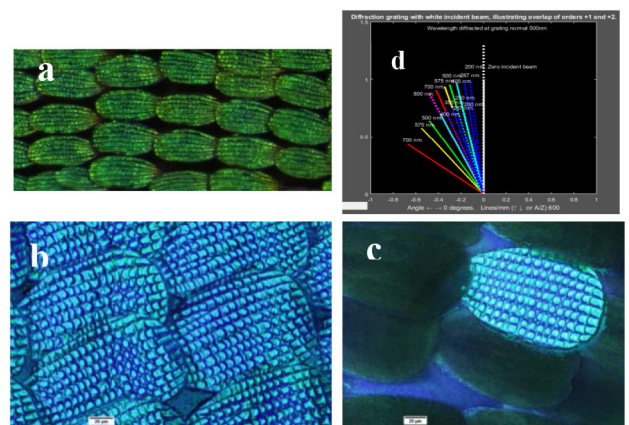

Fig. 4 *Optical microscopy images showing the yellowish-green unpolarised colours at the centre of the scales when illuminated in*
(a) Reflection for normal incident light, *(b, c)* Corresponding polarised images, *(d)* Intensity of the observed colours on the iridescence *Papilio crino*

taking the dark measurement. The WS-2 reference tile reflects light at circa 98% (350–1800 nm) and well suited to quantify the overwhelming reflection of this butterfly in the studied sections.

Secondly, the illumination was oriented toward the wing apex and the collecting probe receives the light that is scattered. Note that some of the scattered light will not be collected by the fibre and transmitted into the spectrometer. Due to instability in the data, the experiment was repeated several times by warming up the light source, taking frequent dark, reference measurements and setting the integration time. For this study, we worked with butterfly *Papilio crino* collected from the Butterfly World Tropical Gardens in Cape Town, South Africa.

As shown in Figs. 5*a* and *b*, the perceived colours of the scattered light changes across the wing with the light incident angles. The spectral reveals double peaks (pronounced peaks at the 45°) which overlays a greenish background. The broad iridescence is centred on a dominate wavelength in the region of 540–560 nm; a wavelength classified as green in the chromatic wavelength. The intensity of peaks increases with increasing incident light angles. In order to explain the colouration mechanism, the transfer method is adopted.
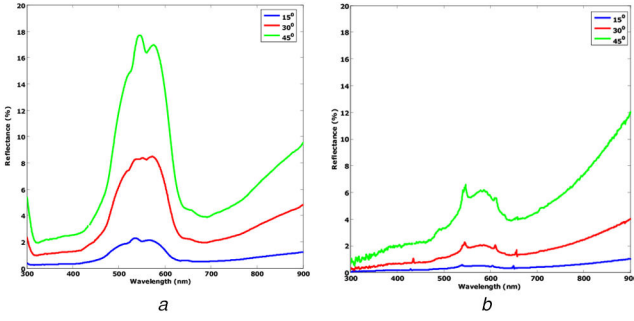
Fig. 5 *Reflectivity spectra of the Papilio crino at*
(a) Left, (b) Right part of the wings under various angles of light incidence

5 Transfer matrix

To analyse the reflection and transmission of light through the double layer stacks (see Fig. 1c) the transfer matrix method [18] is adopted. This is due to the ease of interpreting physical data. Considering the incident, reflected and transmitted waves in the medium, the electric field in the medium is composed of a forward propagating (+) and a back-propagating (−) waves given as (refer [18])

$$\tilde{E} = \tilde{E}_s^{(+)}\hat{s} + \tilde{E}_p^{(+)}\hat{p}^{(+)} + \tilde{E}_s^{(-)}\hat{s} + \tilde{E}_p^{(-)}\hat{p}^{(-)} \tag{1}$$

where $\hat{s}$ and $\hat{p}$ are the unit vectors perpendicular and parallel to the plane of incidence, respectively. The s- and p-polarisation can be described in a 2×1 matrix as $\tilde{E}_{s|p}(z) \equiv \begin{bmatrix} \tilde{E}_{s|p}^{(+)}(z) \\ \tilde{E}_{s|p}^{(-)}(z) \end{bmatrix}$

For a double layer, the transfer matrix can be deduced as in [18] as

$$\tilde{S}_{s|p} = \frac{1}{\tilde{t}_{sp}^{(01)}\tilde{t}_{s|p}^{(12)}\tilde{t}_{s|p}^{(23)}}\begin{bmatrix} 1 & \tilde{r}_{s|p}^{(01)} \\ \tilde{r}_{s|p}^{(01)} & 1 \end{bmatrix} \cdot \begin{bmatrix} e^{-i\gamma_1} & 0 \\ 0 & e^{i\gamma_1} \end{bmatrix}$$
$$\cdot \begin{bmatrix} 1 & \tilde{r}_{s|p}^{(12)} \\ \tilde{r}_{s|p}^{(12)} & 1 \end{bmatrix} \cdot \begin{bmatrix} e^{-i\gamma_2} & 0 \\ 0 & e^{i\gamma_2} \end{bmatrix} \cdot \begin{bmatrix} 1 & \tilde{r}_{s|p}^{(23)} \\ \tilde{r}_{s|p}^{(23)} & 1 \end{bmatrix} \tag{2}$$

$$\tilde{S}_{s|p} = \frac{e^{-1(\tilde{\gamma}_1 + \tilde{\gamma}_2)}}{\tilde{t}_{sp}^{(01)}\tilde{t}_{s|p}^{(12)}\tilde{t}_{s|p}^{(23)}} \begin{bmatrix} \begin{pmatrix} \left(1 + \tilde{r}_{s|p}^{(01)}\tilde{r}_{s|p}^{(12)}e^{i2\gamma_1}\right) \\ +\left(\tilde{r}_{s|p}^{(01)} + \tilde{r}_{s|p}^{(12)}e^{i2\gamma_1}\right)\tilde{r}_{s|p}^{(23)}e^{i2\gamma_2} \end{pmatrix} & \begin{pmatrix} \left(\tilde{r}_{s|p}^{(01)} + \tilde{r}_{s|p}^{(12)}e^{i2\gamma_1}\right) \\ +\left(\tilde{r}_{s|p}^{(01)}\tilde{r}_{s|p}^{(12)} + e^{i2\gamma_1}\right)\tilde{r}_{s|p}^{(23)}e^{i2\gamma_2} \end{pmatrix} \\ \begin{pmatrix} \left(1 + \tilde{r}_{s|p}^{(01)}\tilde{r}_{s|p}^{(12)}e^{i2\gamma_1}\right)\tilde{r}_{s|p}^{(23)} \\ +\left(\tilde{r}_{s|p}^{(01)} + \tilde{r}_{s|p}^{(12)}e^{i2\gamma_1}\right)e^{i2\gamma_2} \end{pmatrix} & \begin{pmatrix} \left(\tilde{r}_{s|p}^{(01)} + \tilde{r}_{s|p}^{(12)}e^{i2\gamma_1}\right)\tilde{r}_{sp}^{(23)} \\ +\left(\tilde{r}_{s|p}^{(01)}\tilde{r}_{s|p}^{(12)} + e^{i2\gamma_1}\right)e^{i2\gamma_2} \end{pmatrix} \end{bmatrix} \tag{3}$$

The reflectivity and transmissivity are expressed as follows:

$$\tilde{r}_{s/p} = \frac{(\tilde{r}_{s/p}^{(01)} + \tilde{r}_{s/p}^{(12)}e^{i2\tilde{\gamma}_1}) + (\tilde{r}_{s/p}^{(01)}\tilde{r}_{s/p}^{(12)} + e^{i2\tilde{\gamma}_1})\tilde{r}_{s/p}^{(23)}e^{i2\tilde{\gamma}_2}}{(1 + \tilde{r}_{s/p}^{(01)}\tilde{r}_{s/p}^{(12)}e^{i2\tilde{\gamma}_1}) + (\tilde{r}_{s/p}^{(12)} + \tilde{r}_{s/p}^{(01)}e^{i2\tilde{\gamma}_1})\tilde{r}_{s/p}^{(23)}e^{i2\tilde{\gamma}_2}} \tag{4}$$

$$\tilde{t}_{s/p} = \frac{(\tilde{t}_{s/p}^{(01)}\tilde{t}_{s/p}^{(12)}\tilde{t}_{s/p}^{(23)}e^{i(\tilde{\gamma}_1 + \tilde{\gamma}_2)})}{(1 + \tilde{r}_{s/p}^{(01)}\tilde{r}_{s/p}^{(12)}e^{i2\tilde{\gamma}_1}) + (\tilde{r}_{s/p}^{(12)} + \tilde{r}_{s/p}^{(01)}e^{i2\tilde{\gamma}_1})\tilde{r}_{s/p}^{(23)}e^{i2\tilde{\gamma}_2}} \tag{5}$$

Rearranging (4) and (5), the reflectivity and transmissivity can be expressed as follows (refer [18]):

$$\tilde{r}_{s|p} = \frac{\tilde{r}_{s|p}^{(01)} + \tilde{r}_{s|p}^{(123)}\exp(i2\tilde{\gamma}_1)}{1 + \tilde{r}_{s|p}^{(01)}\tilde{r}_{s|p}^{(123)}\exp(i2\tilde{\gamma}_1)} \tag{6}$$
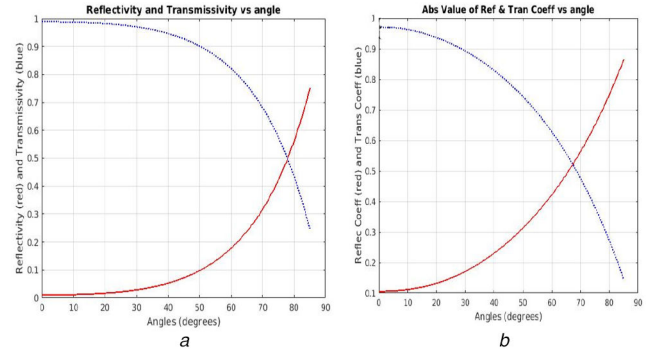

Fig. 6 *Numerical analysis of reflection and transmission of light through the Papilio crino wing*
(a) Plot of reflectivity and transmissivity versus angle, *(b)* Plot of reflection coefficient and transmission coefficient versus angle

$$\tilde{t}_{sp} = \frac{\tilde{t}_{sp}^{(01)}\tilde{t}_{s|p}^{(123)}\exp(i\tilde{\gamma})_1}{1 + \tilde{r}_{s|p}^{(01)}\tilde{r}_{s|p}^{(123)}\exp(i2\tilde{\gamma}_1)} \tag{7}$$

where $r_{s|p}$ is the reflectivity, $t_{s|p}$ is the transmissivity and $\tilde{\gamma}_m = 2\pi\tilde{n}_m\cos(\tilde{\theta})_m dm/\lambda$. λ is known as the vacuum wavelength of the plane wave, m, n are integers.

The optical reflectance on the wings of the *Papilio crino* was determined both experimentally and numerically. Fig. 5 shows the reflectance spectra determined experimentally for (Fig. 5a) left; (Fig. 5b) right parts of the wing. The cuticle multilayer shows reflectance peaks for the left and right wing parts at different angles. These peaks are attributed to the optical interference resulting from the interaction of the incident light with the air-chitin stacks. The left-wing shows higher reflectance values as opposed to the right-wing. This is due to the difference in number as well as the thickness of layers. The maximum wavelength for the peak at 45° angle of light incidence is at $\lambda_{\max} = 555$ nm.

The numerical computation of (5) and (6) is done in stages: (i) considering a single layer, (ii) considering the multilayer and computing the reflection and transmission through the entire system. With each subsequent interface, part of the ray is reflected and part is transmitted. Considering a 2D photonic crystal whose structure parameters are determined from the SEM image shown in Fig. 2a and b, the net reflectivity is the sum of all portions of the single ray that are reflected back into the original medium. The film stack of the *Papilio crino Fabricius* (1792) consists of alternating laminae and air layers. As reported by many authors, the butterfly wing is made of cuticle containing chitin, which has a refractive index of 1.56 [10, 14]. The actual number of air-chitin layers on the butterfly wing is ∼8; thus, the first eight (8) layers were used in the numerical calculation. The results are shown in Fig. 6.

6 Conclusion

The wings of the colourful butterfly; *Papilio crino* was investigated for its colour formation mechanism. The *Papilio crino* butterfly wings have multilayer thin-film structures in their scales, which produce a colourful iridescence from reflected light. In this study, various theoretical and experimental techniques have been proposed to explain the colouration on the wing of *Papilio crino*. The deep concavities as seen on the SEM images aid in the colour appearance of the butterfly. The optical images show the polarisation effects and colour-stimulus synthesis on the wing. Altogether, the theoretical and numerical analysis reveals that the green colouration of *Papilio crino* is due to curved, reflecting multilayers identified on the wing.

Understanding the interaction of light with the wing scale would be an added advantage to develop better interference filters in the thin film industry.

7 Acknowledgment

8 References

[1] Sackey, J., Nuru, Z.Y., Berthier, S.*, et al.*: 'Investigation of nanostructures on the crepuscular 'eyespot' of the *Caligo memnon nymphalidae felder* (1866) butterfly', *Mater. Today, Proc.*, 2015, **2**, (7), pp. 4125–4135

[2] Sackey, J., Nuru, Z.Y., Dompreh, K.A.*, et al.*: 'The study of the structural colouration observed in the *Papilio crino fabricius*, 1792 wings', *J. Nanomed. Nanotechnol.*, 2016, **7**, (387), p. 2

[3] Sackey, J., Nuru, Z.Y., Sone, B.T.*, et al.*: 'Structural and optical investigation on the wings of idea malabarica (Moore, 1877)', *IET Nanobiotechnol.*, 2016, **11**, (1), pp. 71–76

[4] Lee, R.T., Smith, G.S.: 'Detailed electromagnetic simulation for the structural color of butterfly wings', *Appl. Opt.*, 2009, **48**, (21), pp. 4177–4190

[5] Sackey, J., Prevost, P., Dompreh, K.A.*, et al.*: 'Nanostructured characterization of *Papilio demoleus* Linnaeus butterfly wings', *ARM Adv.*, 2018, **3**, pp. 2689–2696

[6] Sackey, J., Dompreh, K.A., Mothudi, B.*, et al.*: 'Theoretical study of electromagnetic transport in Lepidoptera *Danaus plexippus* wing scales', *Heliyon*, 2018, **4**, (1), p. e00502

[7] Wilts, B.D., Michielsen, K., De Raedt, H.*, et al.*: 'Iridescence and spectral filtering of the gyroid-type photonic crystals in *Parides sesostris* wing scales', *Interface. Focus.*, 2011, **2**, pp. 681–687

[8] Tam, H.L., Cheah, K.W., Goh, D.T.*, et al.*: 'Iridescence and nano-structure differences in *Papilio* butterflies', *Opt. Mater. Express*, 2013, **3**, (8), pp. 1087–1092

[9] Gaillot, D.P., Deparis, O., Welch, V.*, et al.*: 'Composite organic-inorganic butterfly scales: production of photonic structures with atomic layer deposition', *Phy. rev. E*, 2008, **78**, (3), p. 031922

[10] Vukusic, P., Sambles, J.R., Lawrence, C.R.: 'Structural colour: colour mixing in wing scales of a butterfly', *Nature*, 2000, **404**, (6777), p. 457

[11] Tada, H., Mann, S.E., Miaoulis, I.N.*, et al.*: 'Effects of a butterfly scale microstructure on the iridescent color observed at different angles', *Appl. Opt.*, 1998, **37**, (9), pp. 1579–1584

[12] Kolle, M., Salgard-Cunha, P.M., Scherer, M.R.*, et al.*: 'Mimicking the colourful wing scale structure of the *Papilio blumei* butterfly', *Nat. Nanotechnol.*, 2010, **5**, (11), p. 511

[13] Crane, J.: 'Spectral reflectance characteristics of butterflies (Lepidoptera) from trinidad', *BWI Zoologica*, 1954, **39**, pp. 85–115

[14] Berthier, S.: '*Iridescences: the physical colors of insects*' (Springer Science & Business Media, Springer-Verlag New York, 2007)

[15] Collins, N.M., Morris, M.G.: '*Threatened swallowtail butterflies of the world*' (IUCN Red Data Book. Iucn., Switzerland, 1985)

[16] Deepika, D.S., Atluri, J.B., Laxmi Sowmya, K.: 'Occurrence and distribution of flying jewels in Visakhapatnam', *Int. J. Adv. Res.*, 2014, **2**, (6), pp. 948–958

[17] Medina, J.M., Nascimento, S.M.C., Vukusic, P.: 'Hyperspectral optical imaging of two different species of Lepidoptera', *Nanoscale Res. Lett.*, 2011, **6**, (1), p. 369

[18] Landry, J. P.: 'Optical oblique-incidence reflectivity difference microscopy: application to label-free detection of reactions in biomolecular microarrays'. University of California, Davis. Appendix B: Reflection and Transmission of Light from Multilayer Films, pp. 321–328, 2008